 doi:10.20944/preprints202012.0561.v1

Article

Rheological Behavior of Blends of Metallocene Catalyzed Long-Chain Branched Polyethylenes. Part I: Shear Rheological and Thermorheological Behavior

Chuangbi Chen, Mehdihasan I. Shekh, Shuming Cui and Florian J. Stadler*

College of Materials Science and Engineering, Shenzhen Key Laboratory of Polymer Science and Technology, Guangdong Research Center for Interfacial Engineering of Functional Materials, Nanshan District Key Laboratory for Biopolymers and Safety Evaluation, Shenzhen University, Shenzhen, 518055, PR China

ORCID:
CCB - 0000-0001-9545-8767, MHS - 0000-0002-8214-6665, SMC - 0000-0002-0514-368X, FJS - 0000-0002-5849-1485

Abstract Long-chain branched metallocene-catalyzed high-density polyethylenes (LCB-mHDPE) were solution blended to obtain blends with varying degrees of branching. A high molecular LCB-mHDPE was mixed with low molecular LCB-mHDPE are varying concentrations, whose rheological behavior is similar but whose molar mass and molar mass distribution is significantly different. Those blends were characterized rheologically to study the effects of concentration, molar mass distribution, and long-chain branching level of the low molecular LCB-mHDPE. Owing to the ultra-long relaxation times of the high molecular LCB-mHDPE, the blends started behaving clearly more long-chain branched than the base materials. The thermorheological complexity showed an apparent increase in the activation energies E_a determined from G', G", and especially δ. $E_a(\delta)$, which for LCB-mHDPE is a peak function, turned out to produce even more pronounced peaks than observed for regular LCB-mPE and also LCB-mPE with broader molar mass distribution. Thus, it is possible to estimate the molar mass distribution from the details of the thermorheological complexity.

Keywords Polyethylene; blend; long-chain branch; thermorheological complexity; activation energy spectrum

Introduction

Polyolefins account for ca. 50% of the synthetic polymers produced worldwide, mainly used for packaging, cable insulation, and household goods. The most commonly used polyolefin is polyethylene (PE), chemically correct also known as polyethene, comprising ca. 30% of the world polymer production, which makes films and cable insulations to a large extent. Both processes include strong elongational deformations, for which strain hardening has proven to be essential for obtaining a stable process and a homogeneous film or layer thickness [1,2].

The strain hardening for classical long-chain branched polyethylene, the well-known low-density polyethylene (LDPE), is established to be very good, while for the Ziegler-Natta polyethylene (linear low (ZN-LLDPE) or high (ZN-HDPE)) usually no strain hardening, at least at high Hencky strain rates [3] $\dot{\epsilon}$ is found [1,2,4,5]. LCB-mPE, shows weak strain hardening, predominantly at low strain rates $\dot{\epsilon}$, making these materials potentially better processable. However, in general the strain hardening of LCB-mPE is not very high, so that the processing behavior is still not entirely on par with LDPE.

In the past, attempts have been made to blend LDPE with LLDPE (ZN-LLDPE, mostly), which has led to a mix of both properties, i.e., the processing improved in comparison to LLDPE, while the mechanical properties degraded.

Preprints (www.preprints.org) | NOT PEER-REVIEWED | Posted: 22 December 2020 doi:10.20944/preprints202012.0561.v1

In the field of analytical characterization of polymers with respect to their branching topography, many attempts were made to characterize the branching structures, which, however, has always suffered from the ambiguity that the effects of long-chain branching and molar mass distribution are very similar to each other in shear rheology so that primitive approaches to characterize samples concerning understanding their long-chain branching topography will not deliver reliable results for polydisperse materials. Classically, the relation between zero shear-rate viscosity η_0 and weight-average molar mass M_w ($\eta_0 \sim M_w^{3.4}$) for linear polymers was found to be molar mass distribution (MMD) independent [6-8]. However, this relation requires the determination of M_w by analytical means, and when taking a ±5% error of M_w-determination into account, only deviations by more than 20% with respect to η_0 can be considered reliable. Further, for many materials determining an accurate M_w is far from straightforward. Furthermore, especially for samples with very broad molar mass distribution, the determination of the true M_w is far from obvious, so that it is not 100% clear whether for some "exotic" molar mass distributions the relation $\eta_0 \sim M_w^{3.4}$ would have to be amended with some MMD-dependent terms [9-12], although the authors believe that it is more likely that this is not the case.

However, another rheological quantity is not dependent on the molar mass distribution, while it reacts to long-chain branching – the thermorheological behavior, as long as it follows an Arrhenius temperature dependence [13-19]. For materials following a WLF-temperature dependence, long-chain branching does not lead to changes in temperature dependence [20].

As already pointed out by Carella, Gotro, and Graessley in 1986 [21], the increase of Arrhenius activation energy is accompanied by thermorheological complexity, i.e., the failure of the time-temperature superposition. Thus, to analyze the temperature dependence of LCB-materials with an Arrhenius temperature dependence, the simplest possible way would be to ignore the thermorheological complexity and make the best fit, which would be scientifically incorrect and would lead to ambiguous results [22]. E.g., the results would depend on the frequency range for which they were calculated. First attempts for a proper analysis of the thermorheological complexity were presented by Carella et al. [21] and Laun [23], who did not analyze the temperature dependence globally but locally, namely by determining the shift factors from specific values of G" and the shear stress σ_{21} (which would be called τ in today's terms), respectively. For LCB-mPE, the thermorheological complexity was first described by Wood-Adams and Costeux through determining activation energies derived from storage modulus G', loss modulus G", the relaxation spectrum, and η_0 [15]. Based on these initial reports, the authors systematically analyzed the thermorheological complexity by determining the rheological spectra with high precision methods [24-26] and shifting them slicewise [27-29]. However, while shifting the relaxation spectrum (and potentially also the retardation spectrum, although to the best of the authors' knowledge that has not been done systematically) is the fundamentally most meaningful way of analyzing such a complicated behavior, it is very cumbersome to do so, as the calculation of a rheological spectrum is a highly difficult undertaking, being easily influenced by various artefacts. Thus doing so is the best but practically rather difficult method.

Instead, research has shown that shifting G', G" and phase angle δ can provide insight into different aspects of the thermorheological complexity of branched LCB-mPE [29,30]. However, at this point, the determination still suffered from the fact that the determination of the shift factors as a function of the rheological quantity (e.g., G', δ) still had to be done manually. For this reason, the authors developed a script, which did that task automatically and more precisely and classified the resulting types of thermorheological complexity [31].

Bai et al.[32] and Shen et al.[33] blended low and high molecular PE with M_w-ratios around 2.5 and 10 and performed a basic rheological characterization, respectively. They found a power-law mixing law; however, based on their data, their materials are linear. Chen et al. [34] made blends of LDPE, LLDPE with an ultrahigh molecular PE and found melt-miscibility but not in solid state. They found thermorheological complexity but did not evaluate it. Chaudhuri et al.[35] melt blended normal HDPE with ultrahigh molecular PE, which was unentangled in order to facilitate melt blending. This resulted in superior blend quality and improved strain hardening.

Preprints (www.preprints.org) | NOT PEER-REVIEWED | Posted: 22 December 2020 doi:10.20944/preprints202012.0561.v1

The thermorheology of polymer blends was investigated for ZN-LLDPE/LDPE and mLLDPE/mVLDPE (very low-density PE) blends by Dordinejad et al. [18,36]. In the case of mLLDPE/mVLDPE-blends, the absence of long-chain branches leads to a small transition between the E_a of each sample, which essentially not thermorheologically complex. However, the LDPE/LLDPE blends show a clear thermorheological complexity, which is systematically changing as a function of composition in a way that at first glance, it is possible to interpolate between the E_a-spectra with respect to G' and δ for each blend by using the pure blend components and a linear mixing rule.

This paper will analyze the rheological behavior of different combinations of blends of long-chain branched mPE, where three different low molar mass LCB-mHDPEs with different molar mass distribution are blended with a high molar mass LCB-mHDPE at different blending ratios. The paper focuses on understanding the interactions in such blends with respect to the thermorheological behavior.

Experimental

Materials and sample preparation

The materials used for blending were synthesized on a laboratory scale by SABIC Limburg B. V. using supported metallocene catalysts. All materials are polyethylene homopolymers (HDPE) to avoid any uncertainties concerning immiscibilities due to different comonomer contents. Table 1 lists the molecular data (M_w, M_z, M_w/M_n, and the LCB-content from SEC-MALLS) of the base materials, showing that they systematically vary the molar mass M_w and molar mass distribution M_w/M_n.

Table 1. molecular data of the base materials.

Materials	M_w [g/mol]	M_z [g/mol]	M_w/M_n [-]	LCB from SEC-MALLS*
HDPE A	87 000	320 000	4.2	medium
HDPE B	105 000	1400 000	15.8	medium-strong
HDPE C	180 000	5400 000	14.1	none
HMW-HDPE 1	460 000	930 000	3.6	weak

* the LCB-content from SEC-MALLS is given qualitatively, only, due to the not 100% constant values obtained from the Zimm-Stockmayer relation [37] and the uncertainties of this relation. Previous rheological investigations have shown that materials that appear linear in SEC-MALLS can have long-chain branches in rheology [38].

The solution method was chosen to avoid the known problem: it is challenging to properly melt-mix two polymers with significantly different viscosity [39].

To reach a total mass of polymer of 5 g, it was calculated how much HDPE (A-C) and HMW-HDPE 1 needed to be mixed. The prepared dry blend was then added into a round bottom flask containing 85ml p-xylene (GC grade). The reflux condensation device was set up and the flask was placed in an oil bath at 120 °C for stirring. The polymers were gradually dissolved, turning the mixture transparent without any visible aggregates within 30 minutes. After stirring for 2 hours, the blend solution was slowly poured into a beaker containing 1.5L deionized water, which was continuously stirred at room temperature for 30 minutes to obtain HDPE polymer flocs. The pouring was performed so that only a thin stream or tiny drops of the solution were added to the stirred water to make the precipitation as fast as possible and avoid possible separation during precipitation. The formed precipitate consisted of fluffy particles with the largest dimension of ca. 2 mm after drying.

The solvent of p-xylene was removed twice by washing with ethanol in a Büchner funnel and then washed with deionized water 3 times. Following this, the blending particles were oven-dried *in vacuo* at 80 °C for 48 hours; afterward, the milky white powder blending samples were obtained.

 doi:10.20944/preprints202012.0561.v1

Table 2 contains the mixture names, which were systematically chosen according to the scheme A-D#, where A-D stands for the low molecular partner HDPE A-D and the number stands for the weight content of HMW-HDPE added. E.g., a mixture of 94% HDPE C and 6% HMW-HDPE is called C6.

Preprints (www.preprints.org) | NOT PEER-REVIEWED | Posted: 22 December 2020 doi:10.20944/preprints202012.0561.v1

Table 2. Designation of the blending materials.

Weight content of HMW-HDPE 1 added	HDPE A	HDPE B	HDPE C
1%	A1	B1	C1
3%	A3	B3	C3
6%	A6	B6	C6
9%	A9	B9	C9
12%	A12	B12	C12

The samples were pressed on a Beijing Future Material vacuum mold pressing machine with different molds. The diameter and thickness of the shear rheological test samples are 25mm and 1-1.5mm, respectively.

Rheology

The rheological characterization was carried out on an Anton Paar MCR 702 rheometer (Graz) equipped with a forced convection oven. All shear rheological experiments were carried out in a nitrogen atmosphere.

The shear rheological experiments consisted of frequency sweeps in the range of ω=100 … 0.1 rad/s and a deformation γ_0 of maximum 5%, which is in the linear range of deformation for all samples. For HMW-HDPE, γ_0=5% proved to be too high, owing to the very high viscosity and, thus, the deformation was lowered to 1%. These experiments were carried out at 150°C, 170°C, 190°C, 210°C, 230°C, and finally repeated at 150°C to confirm that no thermal degradation had taken place. Before each experiment, the temperature was equilibrated within ±0.5K of the desired temperature and followed by a waiting time of 300 s to ensure proper temperature equilibration in the sample.

The obtained data were analyzed in particular for their thermorheological complexity, which was done by the authors' automated method previously [31]. In this method, selected rheological quantities, in our case, storage modulus G', loss modulus G", and phase angle δ are not shifted globally but slicewise to determine the Arrhenius activation energy E_a, i.e., e.g., the activation energy E_a is determined at G'=10000, 5000, and 2000 Pa [15,27]. Practically, a Matlab® script is used to perform the following steps: 1. Fit logG'(logω), logG"(logω), and δ(logω) with 4th or 5th order polynomials, 2. Find the intersection points of these polynomials with a list of constant values of logG', logG", and δ, 3. Determine the E_a for each of those constant values, 4. Plot the data and save the plots and the determined data.

Results

Shear rheological properties

Base materials

The rheological data of the blend components are given in Fig. 1 and show that HDPE A, B, and C, although differing significantly in molar mass, are relatively similar in their rheological behavior. This effect is due to their differences in the degree of long-chain branching and the different molar mass distributions. As shown in Table 1 and Fig. 1, HDPE A is low molecular and has a relatively high degree of long-chain branching, as becomes evident from the high ω_c. Further, it has a non-negligible deviation from the linear reference in the $\delta(|G^*|)$-plot, which is equivalent to the parallelism of G'(ω) and G"(ω) and the almost constant slope of the magnitude of the complex viscosity function $|\eta^*|(\omega)$ for ω<10 rad/s. The relatively narrow molar mass distribution of HDPE A combined with the low M_w=87 kg/mol leads to a relatively early upturn of δ in the $\delta(|G^*|)$-plot. For HDPE B with the somewhat higher M_w=105 kg/mol, the shape of the $\delta(|G^*|)$-plot has changed

Preprints (www.preprints.org) | NOT PEER-REVIEWED | Posted: 22 December 2020 doi:10.20944/preprints202012.0561.v1

significantly. Firstly, the plateau in $\delta(|G^*|)$ is at lower δ, but even more importantly, the signs of an upturn towards the lowest frequencies ω ($\rightarrow$ lowest $|G^*|$) have almost completely disappeared. This becomes more evident when comparing the upturn with that of samples LCB-mHDPE F1 and B2, which were reported before to have almost the same M_w (94 and 102 kg/mol, respectively) but M_w/M_n=2 [40,41], it becomes clear that that the broader molar mass distribution of HDPE A and in particular B leads to significantly broader transitions.

HDPE C is significantly higher in M_w (180 kg/mol) while having almost the same molar mass distribution M_w/M_n=14.1 as HDPE B. The viscosity function $|\eta^*|(\omega)$ for ω<10 rad/s only has a relatively low slope in comparison, so that for the lowest frequencies, $|\eta^*|(\omega)$ of HDPE C is lower than that of HDPE A and B with a higher degree of branching and a much lower molar mass. For comparison with a material with approximately the same M_w but lower M_w/M_n, the LCB-mLLDPE F8B was chosen (M_w=190 kg/mol, M_w/M_n=2, octene content 1.8 mol%) [42,43]. The expected value of zero shear-rate viscosity η_0 for a linear polymer of M_w=180 kg/mol is ca. 80000 Pa s, which is significantly above the viscosity $|\eta^*|(\omega$=0.1 rad/s). For sparsely long-chain branched polymers, in general, the zero shear-rate viscosity η_0 is higher than those of their linear equivalent [44]. Consequently, the high molecular chains must contribute to the viscosity function $|\eta^*|(\omega)$ significantly at much lower frequencies than those measured in this paper.

HMW-HDPE shows an approximately parallel $G'(\omega)$ and $G''(\omega)$ below ω=1 rad/s and a $\delta(|G^*|)$-plot, where δ is decreasing with decreasing ω. Both are typical features of very high molecular LCB-PEs with low to medium long-chain branching [40]. Owing to the high molar mass M_w and the relatively small temperature dependence of PE, it is impossible to reach the terminal regime for such materials within a reasonable time, i.e., within several days [41].

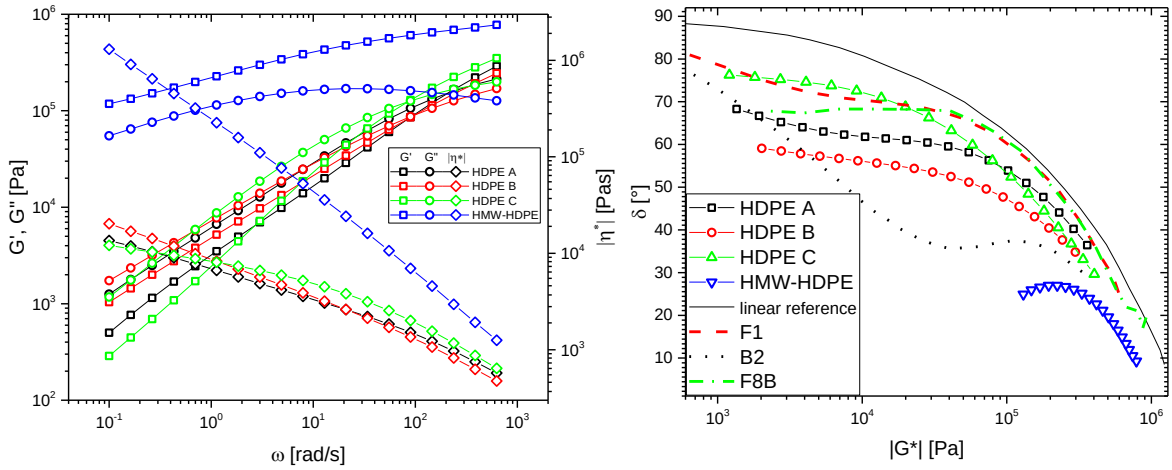

(**a**) (**b**)

Figure 1. a) dynamic-mechanical modulus and viscosity functions of the individual blend components. b) corresponding $\delta(|G^*|)$-plots. The linear reference (black line) was defined elsewhere for HDPEs with M_w/M_n=2-3 [45]. T=150°C, $\gamma_0 \leq 5\%$.

The thermorheological analysis for these samples was conducted following Stadler et al.'s method [31], which will be demonstrated in the following. The temperature-dependent dynamic-mechanical data for HDPE C (Fig. 2) demonstrate that – like usually found for LCB-mPEs – the $G'(\omega)$, $G''(\omega)$, and $|\eta^*|(\omega)$ functions appear to be shiftable at first glance to create a master curve. However, the $\delta(|G^*|)$-plot (Fig. 2b) shows clearly that the data are indeed thermorheologically complex, as in the region plateau, characteristic of LCB-mPE, the $\delta(|G^*|)$-functions are temperature-dependent with the phase angle δ exhibiting lower values at the same complex modulus magnitude $|G^*|$. This sample's behavior, albeit more broad in molar mass distribution, corresponds to a BL-material (LCB-

Preprints (www.preprints.org) | NOT PEER-REVIEWED | Posted: 22 December 2020 doi:10.20944/preprints202012.0561.v1

mPE) typical behavior according to the thermorheological complexity classification scheme [46]. HDPE A and B qualitatively show the same characteristics.

The thermorheological complexity of very high molecular metallocene materials (above M_w=250 kg/mol) has not been reported so far to the best of our knowledge. HMW-HDPE shows an almost temperature-independent viscosity function (Fig. 2e), while the modulus functions show a temperature dependence, which can be explained with the smaller dynamic range and the temperature and frequency dependence of the phase angle. The $\delta(|G^*|)$-plots show that the higher the temperature, the higher is the phase angle δ in the peak around 27°, which occurs before the minimum in the $\delta(|G^*|)$-plot. Based on previous data on comparable materials [40,41,43], this maximum will be followed by a minimum, which in the case of HMW-HDPE is located at too small frequencies to be measured within a reasonable time (>1 day). Taking this somewhat different curve shape into account, it can be concluded that otherwise, HMW-HDPE thermorheologically behaves just like a BL-material (LCB-mPE) according to the thermorheological complexity classification scheme [46].

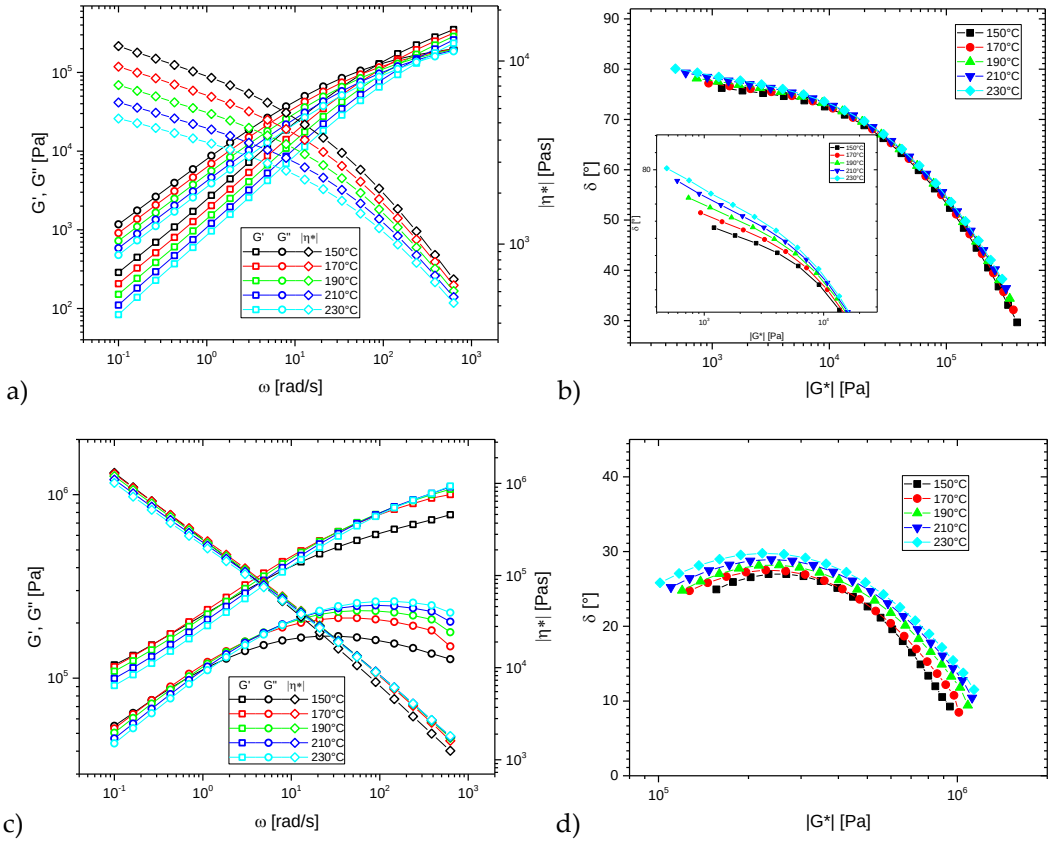

Figure 2. a) dynamic-mechanical modulus and viscosity functions of HDPE C. b) corresponding $\delta(|G^*|)$-plots. c) G′(ω), G″(ω), and |η*|(ω) for HMW-HDPE and d) corresponding $\delta(|G^*|)$-plots. T=150°C, 170°C, 190°C, 210°C, and 230°C color-coded according to the legends. $\gamma_0 \leq 5\%$.

So, in conclusion, HDPE A, B, and C, as well as HMW-HDPE, behave like typical LCB-mPE, albeit with somewhat more smeared out curves, owing to their broader molar mass distribution than previously published data on LCB-mPE.

The thermorheological complexity analysis will be discussed in detail, together with the blends made from those base materials to avoid repetition.

Blends

The frequency-dependent data of the four base materials and 20 blends are given in Fig. 3. In all cases, the addition of the high molecular HMW-HDPE leads to distinct changes in rheological

Preprints (www.preprints.org) | NOT PEER-REVIEWED | Posted: 22 December 2020 doi:10.20944/preprints202012.0561.v1

properties. Even for 1 wt.% HMW-HDPE-content, a clear increase of the viscosity and moduli functions are found at low frequency, which – as expected – is where a high molecular component has the strongest influence.

The HDPE A blends roughly retains the typical shapes of a narrow molar mass distribution LCB-mPE (Fig. 3a,b), characterized by a viscosity function $|\eta^*|(\omega)$ where a more or less constant slope, which then levels of towards the zero shear-rate viscosity η_0 [47], which, however, was not found for any sample in this paper, as the focus was on thermorheological behavior. In the $\delta(|G^*|)$-plot, the addition of HMW-HDPE leads to a decrease of the δ-plateau and further flattening of its slope due to the introduction of long relaxation modes by the blending. These effects are equivalent to each other, as through Kramers-Kronig relations $\delta(\omega)$ and $d\log|\eta^*|/d\log(\omega)$ are inversely proportionally related [47-50]. For the highest HMW-HDPE contents, the $\delta(|G^*|)$-plots start exhibiting a small minimum.

HDPE B and its blends do not show the leveling mentioned above to η_0 and a clear end of the δ-plateau (Fig. 3c,d) due to its broader molar mass distribution. This leads to almost perfectly straight viscosity functions. Consequently, it is nearly impossible to estimate the zero shear-rate viscosity η_0 of these blends. However, previous research on tubular grade polyethylene showed similar behavior so that materials like this possess some relevance in industrial applications.

HDPE C seems to have a lower long-chain branching efficacy than HDPE B, but the same broad molar mass distribution. As a consequence, the viscosity functions are not as straight as for the HDPE B series. However, due to the higher molar mass of HDPE C compared to HDPE B, the terminal relaxation time leads even broader δ-plateaus than the HDPE B blend series. The HDPE C-blend series (except pure HDPE C) does not show a single material whose $\delta(\omega)$ has a negative slope at low ω, i.e., all materials have a maximum at higher frequencies and a minimum at $\omega<0.1$ rad/s. However, the HDPE B-blend series shows such a minimum for B1 and B3, while B6, B9, and B12 show a shape, suggesting that the minimum is very close but not present yet.

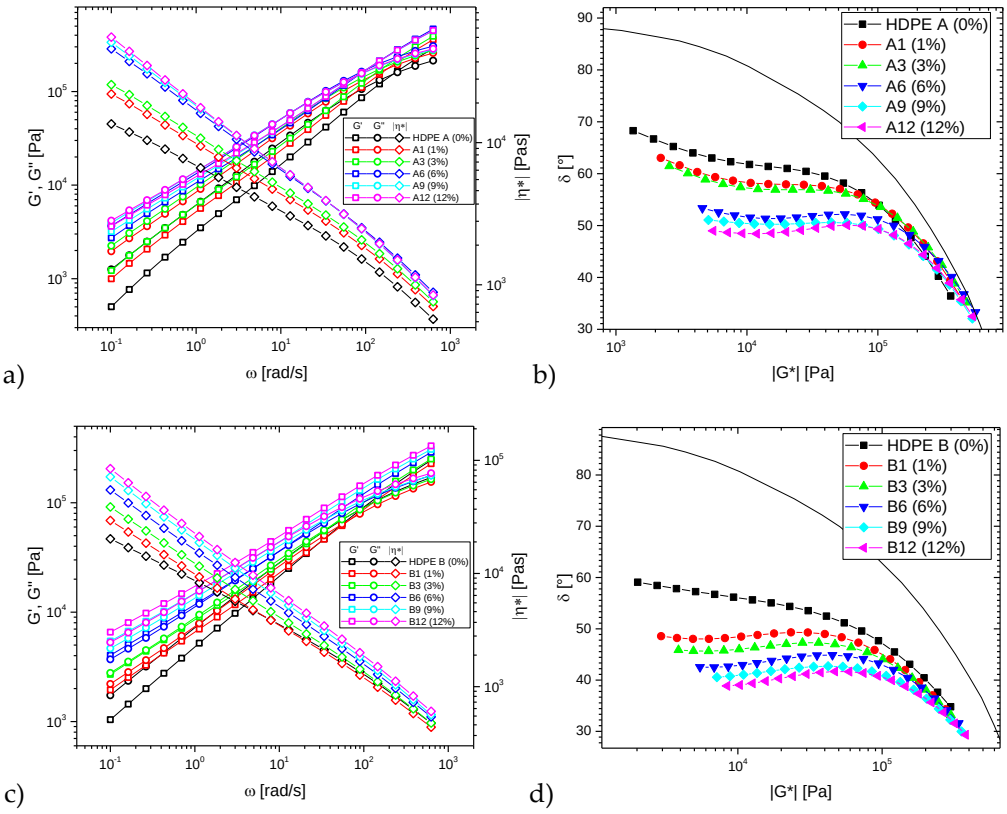

Preprints (www.preprints.org) | NOT PEER-REVIEWED | Posted: 22 December 2020 doi:10.20944/preprints202012.0561.v1

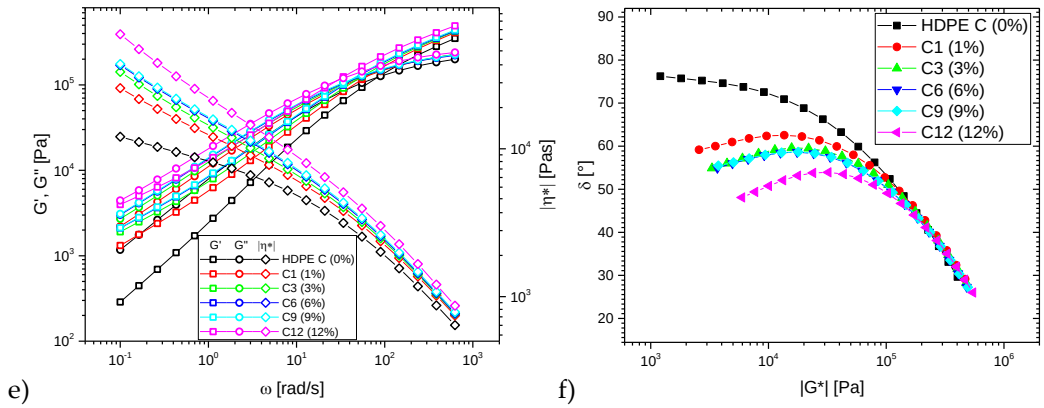

Figure 3. a) dynamic-mechanical modulus and viscosity functions of the blends of a) HDPE A, c) HDPE B, and e) HDPE C. Corresponding $\delta(|G^*|)$-plots for b) HDPE A, d) HDPE B, and f) HDPE C. T=150°C, γ_0=<5%.

The dependence of the HMW-content c dependent crossover frequencies ω_c for the blends (Fig. 4) show a clear decrease with increasing c. Considering that ω_c is proven to be related to M_w [7,51], it is not surprising that blending HMW-HDPE will increase M_w and, thus, also ω_c. However, these correlations between ω_c (or $1/\lambda=\omega_c$) and M_w are influenced by various factors, most notably by the molar mass distribution. The molar mass distribution changes when blending two materials, and, thus, the relationship is not quantitatively analyzed. However, it is clear that $\omega_c(c)$ (Fig. 4a) shows a common trend for all blend series. It should be noted that those correlations between ω_c (or $1/\lambda$) and M_w have been established for linear and not for long-chain branched PE. However, as long as the deviation from the linear relation (as shown in Fig. 3) is not significant for δ<50°C, it is safe to relate ω_c with M_w, which is in line with fits of the viscosity functions of narrow molar mass distribution LCB-mPEs [52]. This becomes clear for the sample C12, whose δ(ω)-function exhibits a peak around 52° before decreasing again with decreasing ω. B12 has a very similar behavior but does not exceed 45°, thus does not have a crossover frequency ω_c.

When normalizing ω_c on the value found for the pure low molecular blend partner, it becomes clear that, although somewhat scattered, the slope of the decrease function is independent of the base material, which is surprising, considering that the molar mass M_w ratios of the blends' base materials are between 5.4 for the HDPE A-HMW-HDPE and 2.6 for the HDPE C-HMW-HDPE blend series.

If we assume that the materials are monodisperse and that the crossover frequency ω_c is only related to M_w, it would be possible to calculate the expected M_w and thus ω_c ($\sim M_w^{3.6}$) simply from the constituents' M_w and contents. Consequently, the HDPE A series ω_c should decrease to $\omega_c/\omega_c(c=0$ wt.%) ≈0.21 and for HDPE C to ≈0.40 for c=12 wt.%. However, such a big difference is not found for the blends, which indicates that the influence of molar mass distribution on blends needs a lot more understanding that cannot be broken down to such a primitive approach.

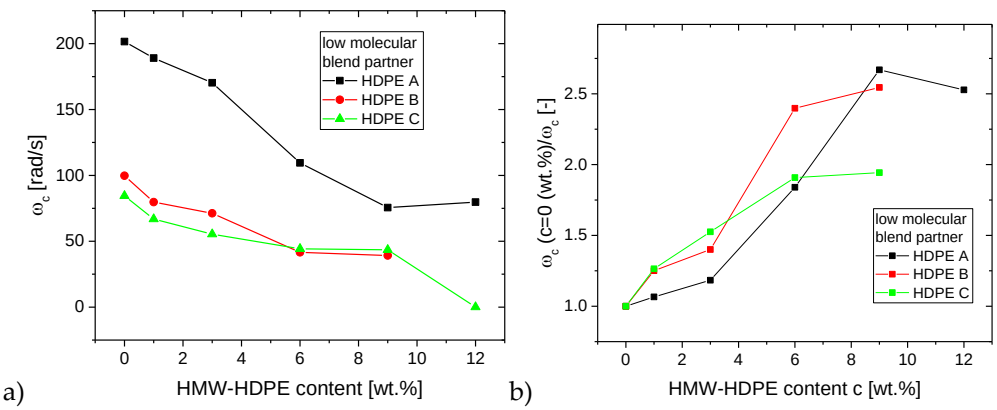

Preprints (www.preprints.org) | NOT PEER-REVIEWED | Posted: 22 December 2020 doi:10.20944/preprints202012.0561.v1

Figure 4. a) crossover frequencies ω_c for the blends as a function of HMW-HDPE content c, b) ω_c normalized to ω_c of the pure low molecular blend partner.

The differences become much more pronounced when looking at the lowest frequencies, however (Fig. 5). The $\delta(|G^*|)$-plots only for ω =0.1 rad/s show a clearly decreasing trend for the phase angle δ, while the complex modulus $|G^*|$ increases monotonously (Fig. 5a). While the data for the HDPE A-C blends are relatively similar, for the HDPE D blends, the increase in $|G^*|$ is very small. The complex viscosity $|\eta^*|$ at ω =0.1 rad/s as a function of HMW-HDPE content normalized to the low molecular blend partners' $|\eta^*|$, shows an increase by about factor 4 for the HDPE A-C blends (Fig. 5b).

Fig. 5c shows the dependence of phase angle δ on HMW-HDPE content c, which for larger c leads to an almost parallel dependence, while for small c, the initial decrease of $\delta$is very much sample dependent.

This indicates that at the low frequencies, even a tiny amount of HMW-HDPE in the blends has a significant effect on the viscoelastic behavior, which is qualitatively in line with the strong increase of the elastic compliance found by Münstedt [53]. Further, it indicates that the larger the molar mass difference is, the larger is the effect on the rheological properties, especially at low frequency.

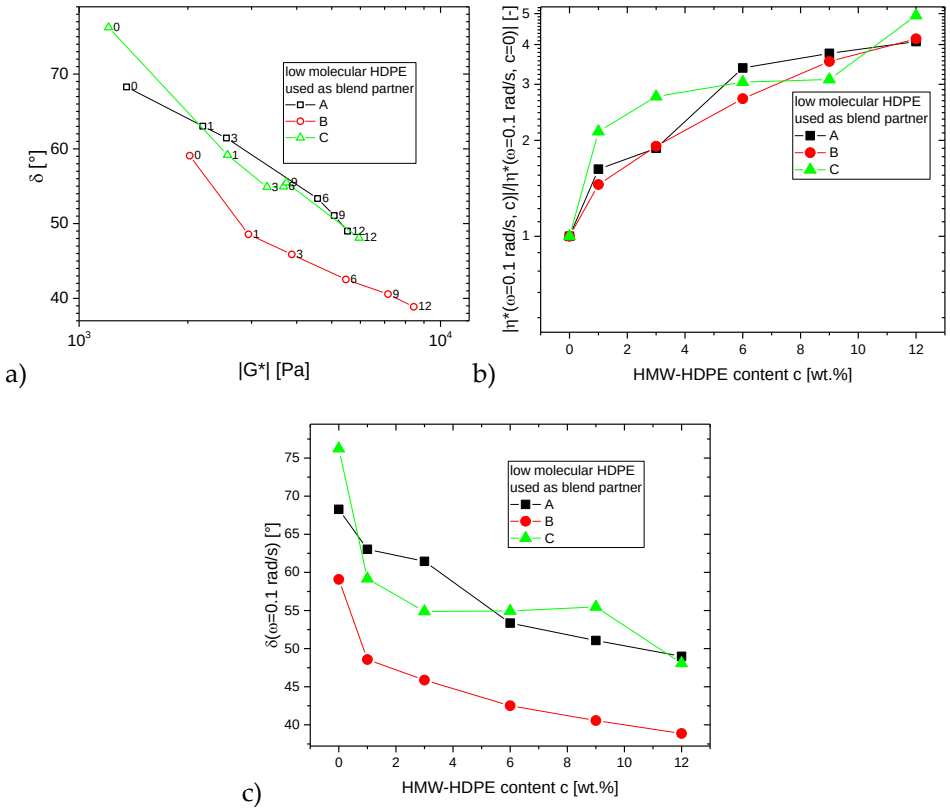

Figure 5. comparison of the data obtained for the blends at ω=0.1 rad/s and T=150°C. a) $\delta(|G^*|)$-plot, b) viscosity change normalized to viscosity of low molecular blend partner $|\eta^*(\omega$ =0.1 rad/s, c)|/|η*(ω=0.1 rad/s, c=0)|, c) δ(ω=0.1 rad/s).

Thermorheological behavior

The analysis method for the thermorheological behavior was described in detail before[31] and will, therefore, not be repeated here. The results of the automated analysis of the thermorheological complexity are given in Fig. 6a-c. $E_a(G')$ (Fig. 6a) shows that blending HDPE A with HMW-HDPE leads to an overall increase of E_a up to 6% HMW-HDPE-content c. Above this threshold, the activation energies above 30 kJ/mol are decreasing. For all samples, the data exhibits a maximum in $E_a(G')$,

Preprints (www.preprints.org) | NOT PEER-REVIEWED | Posted: 22 December 2020 doi:10.20944/preprints202012.0561.v1

whose G'-position increases with increasing HMW-HDPE-content c, i.e., the influence of the long-chain branches becomes visible at higher G', which also corresponds to higher ω.

The loss modulus activation energy spectrum $E_a(G'')$ shows an increase of E_a towards decreasing G", which is due to the increasing efficacy of long-chain branches towards low frequencies (=long relaxation times) [30]. Increasing the blend concentration c leads to an overall increase of $E_a(G'')$ while mostly retaining the shape of the loss modulus activation energy spectrum.

Like in previous reports, we also found that $E_a(G')$ and $E_a(G'')$ is "too low" for high G' and G", i.e., the observed values of E_a are significantly below the expected value of E_a for linear HDPE (27 kJ/mol). In previous papers, it was also found for the relaxation strength activation energy spectrum $E_a(H)$ [27,28]. This effect is not found for linear materials when evaluating it with the same method; thus, it is most likely not any form of experimental artifact. However, so far, nobody has presented a conclusive mechanism for observing such "too low" E_a, and we also have not found a credible explanation for this effect, which is why regrettably, we have to keep this question open.

The activation energy spectra with respect to δ $E_a(\delta)$ shows a clear peak function (Fig. 6c), which increases in peak heights with the increase in HMW-HDPE-content c, while δ_{max}, which has been proven to be closely related to the characteristic phase angle δ_c, according to the definition of Trinkle et al.[54,55], decreases with increasing c. Those effects are expected, as adding HMW-HDPE leads to an increase in long relaxation times, which – in general – broadens the relaxation spectrum and, thus, leads to increased elasticity, i.e., a lower plateau in the $\delta(|G^*|)$-plot or $\delta(\omega)$-plot. However, unlike for "normal LCB-mPE", a decrease in δ_{max} is usually accompanied by a moderate increase in the peak activation energy of $E_a(\delta)$ of $E_{a,max}$. The values $E_{a,max}$ and δ_c found for HDPE A are 91.7 kJ/mol and 63.5°, respectively, which is in good agreement to previously reported values for similar materials [31]. However, the blends show much higher values of $E_{a,max}$ than expected, which is counterintuitive at first glance, as adding an HMW-HDPE broadens the molar mass distribution, which according to previously reported results, "smears out the plateaus" in the $\delta(|G^*|)$-plot or $\delta(\omega)$-plot and thus should rather decrease than increase $E_{a,max}$.

It should be mentioned that due to the piecewise evaluation, the activation energies are highly influenced by their input. In the plateau regime of δ(ω), the values of $E_a(\delta)$ can increase significantly beyond the values of $E_a(G')$ *and* $E_a(G'')$. This is, of course, not supposed to be taken as a physically valid value but rather as an indication that is very valuable for branching analysis.

Fig. 6d and e show a comparison of the $\delta(\omega)$-plots of HDPE A and A3. In these plots, the position of $E_{a,max}$ is marked by the horizontal line, and the pink x marks the points where the data cross it. Further, the other material's corresponding values are given in the respective plots as small black x to illustrate the differences better. The comparison between these two samples, differing by the 3% addition of HMW-HDPE, leads to significant differences in the phase angle functions $\delta(\omega)$. Namely, the plateau of A3 is significantly widened and flattened to the extent that for 150°C, an almost constant value of δ is found for ω= 1 … 10 rad/s. As a consequence, the spread between the data at 150°C and 230°C at δ=59° is significantly larger than the corresponding spread for HDPE A at δ=63°. In both cases, the value was taken at δ_{max}, i.e., where $E_a=E_{a,max}$.

Thus, the high molecular tail introduced by blending leads to significantly different behavior than found for the "normal" broadly distributed LCB-mPE. The high molecular tail stemming from 1-12% HMW-HDPE, which in the case of HDPE A is 5.4 times higher with respect to M_w, leads to a significant lengthening of the terminal relaxation time and to an increase in perceived LCB-efficacy.

For higher HMW-HDPE contents than 3%, some erratic peak functions were found, resulting from $\delta(\omega)$ exhibiting a minimum, as can be seen from Fig. 3a,b. As the evaluation routine finds one frequency, at which the phase angle δ is exactly z°, the analysis is not adequately defined, as the slice-wise evaluation assumes that all evaluated functions are monotonically increasing or decreasing. For this reason, the values found for samples having a minimum in $\delta(\omega)$ cannot be trusted in the regime of the minimum, which is indicated by the gray ellipse in Fig. 6c.

Despite these limitations owing to the slice-wise evaluation approach, it is possible to determine $E_{a,max}$ for A6 and A9 but not for A12, whose δ-minimum is too pronounced to yield reliable values. $E_{a,max}$ of A6 and A9 are around 160 kJ/mol, which is beyond any E_a reported for thermorheologically

Preprints (www.preprints.org) | NOT PEER-REVIEWED | Posted: 22 December 2020 doi:10.20944/preprints202012.0561.v1

complex polyethylene. This illustrates the strong effect of the broadening of the spectrum by blending yielding bimodal materials. Fig. 6e clearly shows that δ(ω) of A3 at 150°C has a plateau (dδ/dlogω=0), while at 230°C, the smallest slope is around 2.6, as can be seen from the phase angle derivative plots (dδ/dlogω(ω), Fig. 6d,e). For HDPE A (Fig. 6d) the corresponding minima are 1.6 and 3.5, respectively. The higher the HMW-HDPE-content c, the more negative is the minimum slope, which leads to increased $E_{a,max}$ and at the same time to a failure of the method, as a minimum in δ(ω) (dδ/dlogω<0) means that more than a certain δ is reached at more than one ω.

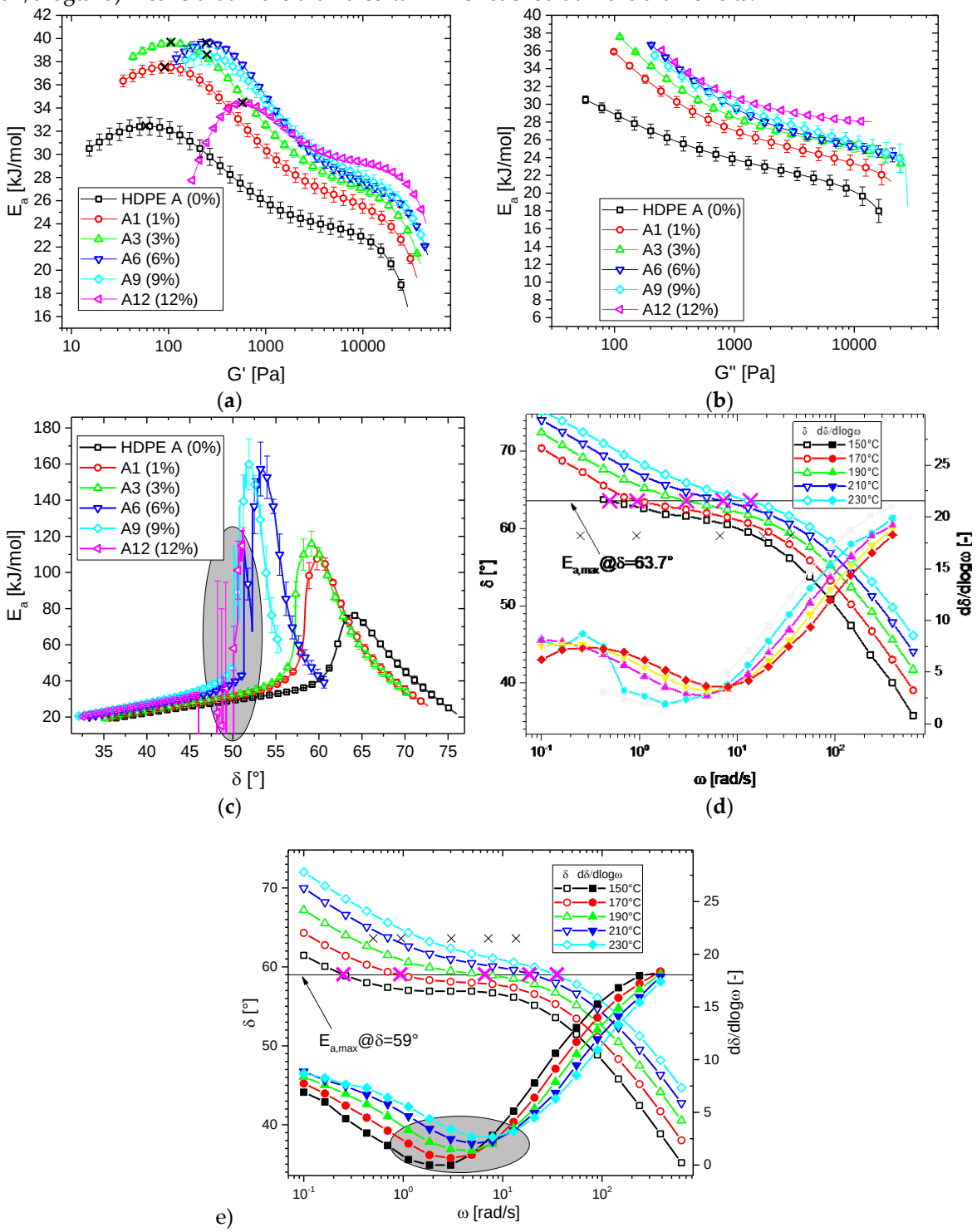

Figure 6. activation energy spectra of a) storage modulus ($E_a(G')$), b) loss modulus ($E_a(G'')$), and c) phase angle ($E_a(\delta)$). D) δ(ω) of HDPE A, e) δ(ω) of A3.

Preprints (www.preprints.org) | NOT PEER-REVIEWED | Posted: 22 December 2020 doi:10.20944/preprints202012.0561.v1

For these reasons, the thermorheological complexity of the other blend series is only discussed in terms of $E_a(G')$ and $E_a(\delta)$. The plots of the other quantities are given in supplementary information.

Fig. 7 shows $E_a(G')$ and $E_a(\delta)$ of the blend series B-D. The HDPE B blend series shows the largest similarity to the HDPE A blend series (Fig. 7a,b). Compared to the HDPE A blend series, the higher molar mass and longer terminal relaxation time of the HDPE B blend series makes the storage modulus activation energy spectrum $E_a(G')$ end at higher G'. This and the higher branching efficacy of HDPE B vs. HDPE A make the samples approach higher E_a-values as seen from the higher slopes found when approaching the maximum. Further, the deviation from the E_a of linear materials (ca. E_a=27 kJ/mol) occurs at somewhat higher G'. $E_a(\delta)$ clearly shows that the typical peak shifts towards lower δ with increasing c. However, only for the purse HDPE B, a regular $E_a(\delta)$ peak could be found. A minimum in $\delta(\omega)$ exists for all blends, which, as discussed before, leads to extremely high $E_{a,max}$ and erratic peak shapes. Thus, the obtained values for e.g., $E_{a,max}$ cannot be considered quantitative, but it can be concluded that they are very high and that δ_{max} decreases with increasing c.

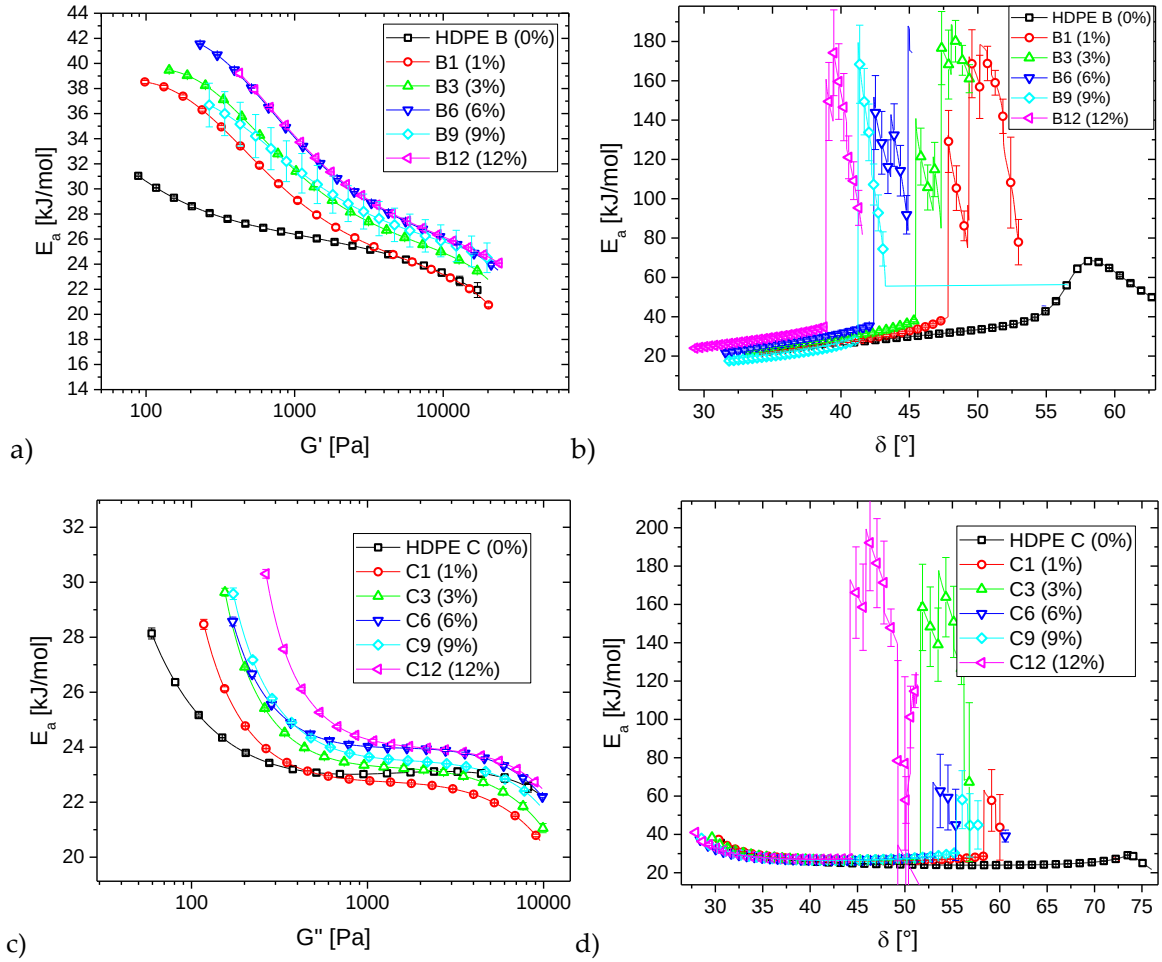

Figure 7. activation energy spectra of a), c) storage modulus ($E_a(G')$), b), d) phase angle ($E_a(\delta)$) of a), b) HDPE B blend series, c), d) HDPE C blend series.

Previously, it was established that LCB-mPE with narrow molar mass distribution (BL, blue downward-pointing triangles) have a significantly higher $E_{a,max}(\delta_{max})$ than LCB-mPE with a broader molar mass distribution (dark blue upward-pointing triangles), whose $E_{a,max}(\delta_{max})$ is rather close to tubular and especially autoclave LDPE [31]. It was then possible to accumulate some more data, particularly for the LDPE-LLDPE blends of Dordinejad and Jafari [25], which were analyzed with the same standard analysis method. This data set shows a transition from LDPE-like behavior (BH) for the LDPE-rich blends to LCB-mPE like behavior (BL). The LLDPE used was a Ziegler-Natta grade,

Preprints (www.preprints.org) | NOT PEER-REVIEWED | Posted: 22 December 2020 doi:10.20944/preprints202012.0561.v1

but according to the data published somewhat, long-chain branched, making it sufficiently similar to a slightly branched LCB-mPE.

When comparing the previously obtained data to the LCB-mPE blends, it becomes immediately obvious that the special curve shape of $\delta(\omega)$ leads to $E_{a,max}(\delta_{max})$ very different from previously known samples, owing to their very high $E_a(\delta)$-peaks. This confirms the unusual behavior of the LCB-mPE blends, which is due to the bimodal molar mass distribution with long-chain branches in the high molecular tail.

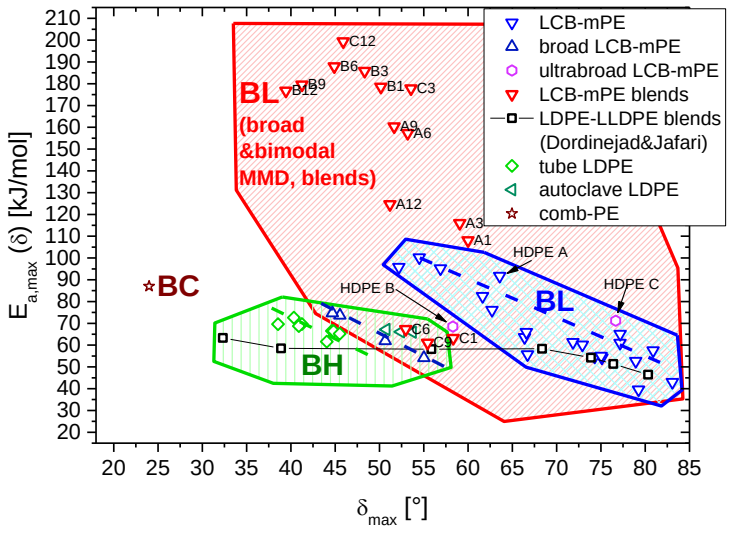

Figure 8. plot of $E_{a,max}$ vs. δ_{max} for the samples in comparison with previously characterized samples. The samples included in this paper are denoted with their sample designation.

Besides the discussion of $E_a(\delta)$, also $E_a(G')$ can give us interesting insights into the rheological behavior. When looking at Fig. 6a and Fig. 7a,c, and e carefully, the point at which the samples have a clear upturn in $E_a(G')$ depends on both types of low molecular blend partner and blend composition. To analyze this behavior better, the turning points were determined for each sample and the G′ component of the inflection point is given in Fig. 9.

Two trends are immediately visible: firstly, an increase of HMW-HDPE content leads to an increased inflection point, i.e., the activation energy E_a increases at a higher storage modulus beyond the level of linear material. Thus, the influence of the long-chain branches appears at higher G′ and, consequently, at higher ω. This effect is exceptionally well visible at low HMW-HDPE contents. This is in agreement with observations of Münstedt [53] of minute amounts of a high molecular component having a massive influence on the elasticity of a blend, for which G′ is the indicator used in this paper.

Secondly, the higher the molar mass of the low molecular material, the lower the G′ at which the inflection point curves are found. This trend can be understood only to be the consequence of the combination of several parameters. Firstly, as the HMW-HDPE is the same for all materials, a higher molar mass of the low molecular HDPE means that both blend components' molar mass ratio is HDPE A-blends> HDPE B-blends> HDPE C-blends. The difference between the low molecular base polymers HDPE A, HDPE B, and HDPE C is primarily in M_w, M_w/M_n, and the LCB-content, which balances out the differences in molar mass, as the viscosity functions of the three base materials are very similar (Fig. 1). The lower LCB-content of HDPE B and HDPE C leads to an inflection point at rather low G′, which means that the long-chain branches are more or less not showing until relatively low ω. That can be explained by their lower concentration and the higher average molar mass, which means that many longer chains need to relax along the sparser LCB-chains, which are the key contributors to a higher E_a.

Preprints (www.preprints.org) | NOT PEER-REVIEWED | Posted: 22 December 2020 doi:10.20944/preprints202012.0561.v1

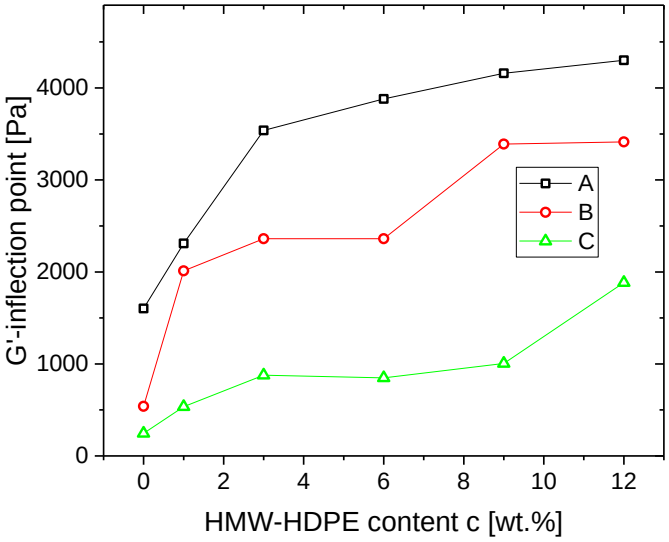

Figure 9. $E_a(G')$-inflection point plotted as a function of HMW-HDPE content c [wt.%].

Conclusions

Blends of 2 LCB-mPEs with different molar masses and molar mass distributions were created by solution blending. The rheological analysis revealed that the blends' behavior has already changed significantly when adding a minute amount of high molecular material.

A high molecular HDPE lowers the phase angle at low frequency systematically, which suggests an increased elasticity and an extended terminal relaxation time. The samples' thermorheological complexity varied systematically with the content of HMW-HDPE. Due to the change of the curve shape of $\delta(\omega)$, the shape of the phase angle activation energy spectrum $E_a(\delta)$ changed significantly as well. The long relaxation times introduced by HMW-HDPE led to a clear flattening or even the appearance of a minimum in $\delta(\omega)$ at intermediate δ (30-60°, depending on the material), which leads to very high E_a in the region of this plateau or minimum.

This is very different from previously observed behavior for normal LCB-mPE with M_w/M_n≈2-3 and broad molar mass distribution LCB-mPE with M_w/M_n≈4-6, whose $E_{a,max}$. For those previously established materials, $E_{a,max}$ was found to be between 50 and 100 kJ/mol, depending on the maximum activation energy phase angle δ_{max} (approximately the same as the characteristic phase angle δ_c) and an increase in M_w/M_n led to a significant decrease of $E_{a,max}$ for those broad LCB-mPEs, whose molar mass distribution is unimodal. For the bimodal samples characterized in this paper, $E_{a,max}$ is much higher, despite the much broader molar mass distribution, which is the consequence of the bimodal molar mass distribution introducing very long relaxation times, leading to $E_{a,max}$ up to 200 kJ/mol. Therefore, it is concluded that the molar mass distribution M_w/M_n alone (of course together with the LCB-content and distribution) does not determine the thermorheologically complex behavior but that the shape of the molar mass distribution matters as well in combination with the LCB-distribution, which together determine the relaxation spectrum and, thus, the viscoelastic functions.

Acknowledgments

The work was supported by SABIC Netherlands through providing the samples and characterization for this publication and to provide funding for a joint project, whose results are partially contained in here.

Contributions

Rheological experiments – CCB, FJS, CSM, blend preparation – CCB, MHS, data analysis - CCB, FJS, conceptualization – FJS, writing of initial draft – FJS, CCB, supervision - FJS

References

1. Münstedt, H.; Steffl, T.; Malmberg, A. Correlation between rheological behaviour in uniaxial elongation and film blowing properties of various polyethylenes. *Rheologica Acta* **2005**, *45*, 14-22, doi:10.1007/s00397-005-0435-6.
2. Münstedt, H.; Kurzbeck, S.; Stange, J. Importance of elongational properties of polymer melts for film blowing and thermoforming. *Polym Eng Sci* **2006**, *46*, 1190-1195, doi:10.1002/Pen.20588.
3. Hencky, H. Über die Form des Elastizitatsgesetzes bei ideal elastischen Stoffen. *Zeitschrift für technische Physik* **1928**, *9*, 215-220.
4. Stadler, F.J.; Kaschta, J.; Münstedt, H.; Becker, F.; Buback, M. Influence of molar mass distribution and long-chain branching on strain hardening of low density polyethylene. *Rheologica Acta* **2009**, *48*, 479-490, doi:10.1007/s00397-008-0334-8.
5. Stadler, F.J.; Nishioka, A.; Stange, J.; Koyama, K.; Münstedt, H. Comparison of the elongational behavior of various polyolefins in uniaxial and equibiaxial flows. *Rheol Acta* **2007**, *46*, 1003-1012, doi:10.1007/s00397-007-0190-y.
6. Berry; Fox. The viscosity of polymers and their concentrated solutions. *Adv. Polymer Sci.* **1968**, *5*, 261--357.
7. Stadler, F.J.; Piel, C.; Kaschta, J.; Rulhoff, S.; Kaminsky, W.; Münstedt, H. Dependence of the zero shear-rate viscosity and the viscosity function of linear high-density polyethylenes on the mass-average molar mass and polydispersity. *Rheol Acta* **2006**, *45*, 755-764, doi:10.1007/s00397-005-0042-6.
8. Stadler, F.J.; Münstedt, H. Terminal viscous and elastic properties of linear ethene / α -olefin copolymers. *Journal of Rheology* **2008**, *52*, 697, doi:10.1122/1.2892039.
9. Otegui, J.; Ramos, J.; Vega, J.F.; Martinez-Salazar, J. Effect of high molar mass species on linear viscoelastic properties of polyethylene melts. *Eur Polym J* **2013**, *49*, 2748-2758, doi:10.1016/j.eurpolymj.2013.06.015.
10. Ansari, M.; Hatzikiriakos, S.G.; Sukhadia, A.M.; Rohlfing, D.C. Rheology of Ziegler–Natta and metallocene high-density polyethylenes: broad molecular weight distribution effects. *Rheologica Acta* **2010**, *50*, 17-27, doi:10.1007/s00397-010-0503-4.
11. Vega, J.F.; Otegui, J.; Ramos, J.; Martínez-Salazar, J. Effect of molecular weight distribution on Newtonian viscosity of linear polyethylene. *Rheologica Acta* **2011**, *51*, 81-87, doi:10.1007/s00397-011-0594-6.
12. Wasserman, S.H.; Graessley, W.W. Prediction of linear viscoelastic response for entangled polyolefin melts from molecular weight distribution. *Polym Eng Sci* **1996**, *36*, 852-861, doi:10.1002/Pen.10472.
13. Mavridis, H.; Shroff, R.N. Temperature-Dependence of Polyolefin Melt Rheology. *Polym Eng Sci* **1992**, *32*, 1778-1791.
14. Carella, J.M. Comments on the Paper “Comparison of the Rheological Properties of Metallocene-Catalyzed and Conventional High-Density Polyethylenes”. *Macromolecules* **1996**, *29*, 8280-8281, doi:S0024-9297(96)00909-6.
15. Wood-Adams, P.; Costeux, S. Thermorheological Behavior of Polyethylene: Effects of Microstructure and Long Chain Branching. *Macromolecules* **2001**, *34*, 6281-6290, doi:10.1021/ma0017034.

16. Lohse, D.J.; Milner, S.T.; Fetters, L.J.; Xenidou, M.; Hadjichristidis, N.; Mendelson, R.A.; Garcia-Franco, C.A.; Lyon, M.K. Well-defined, model long chain branched polyethylene. 2. Melt rheological behavior. *Macromolecules* **2002**, *35*, 3066-3075, doi:10.1021/Ma0117559.
17. Mohammadi, M.; Yousefi, A.A.; Ehsani, M. Thermorheological analysis of blend of high- and low-density polyethylenes. *Journal of Polymer Research* **2012**, *19*, doi:10.1007/s10965-011-9798-9.
18. Dordinejad, A.K.; Jafari, S.H. A qualitative assessment of long chain branching content in LLDPE, LDPE and their blends via thermorheological analysis. *J Appl Polym Sci* **2013**, *130*, 3240-3250, doi:10.1002/app.39560.
19. Derakhshandeh, M.; Ansari, M.; Doufas, A.K.; Hatzikiriakos, S.G. Microstructure characterization of polyethylene using thermo-rheological methods. *Polymer Testing* **2017**, *60*, 68-77, doi:10.1016/j.polymertesting.2017.03.010.
20. Hepperle, J.; Münstedt, H.; Haug, P.K.; Eisenbach, C.D. Rheological properties of branched polystyrenes: linear viscoelastic behavior. *Rheologica Acta* **2005**, *45*, 151-163, doi:10.1007/s00397-005-0033-7.
21. Carella, J.M.; Gotro, J.T.; Graessley, W.W. Thermorheological Effects of Long-Chain Branching in Entangled Polymer Melts. *Macromolecules* **1986**, *19*, 659-667, doi:10.1021/ma00157a031.
22. Kokko, E.; Malmberg, A.; Lehmus, P.; Lofgren, B.; Seppala, J.V. Influence of the catalyst and polymerization conditions on the long-chain branching of metallocene-catalyzed polyethenes. *J Polym Sci Pol Chem* **2000**, *38*, 376-388, doi:10.1002/(Sici)1099-0518(20000115)38:2<376::Aid-Pola12>3.0.Co;2-5.
23. Laun, H.M. Orientation of macromolecules and elastic deformations in polymer melts. Influence of molecular structure on the reptation of molecules. *Progress in Colloid Polymer Science* **1987**, *75*, 111-139 (DOI: 110.1007/BFb0109414), doi:10.1007/BFb0109414.
24. Stadler, F.J.; Bailly, C. A new method for the calculation of continuous relaxation spectra from dynamic-mechanical data. *Rheol Acta* **2009**, *48*, 33-49, doi:10.1007/s00397-008-0303-2.
25. Kaschta, J.; Stadler, F.J. Avoiding waviness of relaxation spectra. *Rheol Acta* **2009**, *48*, 709-713, doi:10.1007/s00397-009-0370-z.
26. Stadler, F.J. Effect of incomplete datasets on the calculation of continuous relaxation spectra from dynamic-mechanical data. *Rheol Acta* **2010**, *49*, 1041-1057, doi:10.1007/s00397-010-0479-0.
27. Stadler, F.J.; Kaschta, J.; Münstedt, H. Thermorheological Behavior of Various Long-Chain Branched Polyethylenes. *Macromolecules* **2008**, *41*, 1328-1333, doi:10.1021/ma702367a.
28. Kessner, U.; Kaschta, J.; Stadler, F.J.; Le Duff, C.c.S.; Drooghaag, X.; Münstedt, H. Thermorheological Behavior of Various Short- and Long-Chain Branched Polyethylenes and Their Correlations with the Molecular Structure. *Macromolecules* **2010**, *43*, 7341-7350, doi:10.1021/ma100705f.

29. Resch, J.A.; Keßner, U.; Stadler, F.J. Thermorheological behavior of polyethylene: a sensitive probe to molecular structure. *Rheol Acta* **2011**, *50*, 559-575, doi:10.1007/s00397-011-0575-9.
30. Kessner, U.; Kaschta, J.; Münstedt, H. Determination of method-invariant activation energies of long-chain branched low-density polyethylenes. *J Rheol* **2009**, *53*, 1001-1016, doi:10.1122/1.3124682.
31. Stadler, F.J.; Chun, Y.S.; Han, J.H.; Lee, E.; Park, S.H.; Yang, C.B.; Choi, C. Deriving comprehensive structural information on long-chain branched polyethylenes from analysis of thermo-rheological complexity. *Polymer* **2016**, *104*, 179-192, doi:10.1016/j.polymer.2016.07.084.
32. Bai, L.; Li, Y.-M.; Yang, W.; Yang, M.-B. Rheological Behavior and Mechanical Properties of High-Density Polyethylene Blends with Different Molecular Weights. *J Appl Polym Sci* **2010**, *118*, 1356-1363, doi:10.1002/app.32329.
33. Shen, H.-W.; Xie, B.-H.; Yang, W.; Yang, M.-B. Thermal and rheological properties of polyethylene blends with bimodal molecular weight distribution. *J Appl Polym Sci* **2013**, *129*, 2145-2151, doi:10.1002/app.38850.
34. Chen, Y.; Zou, H.; Liang, M.; Liu, P. Rheological, thermal, and morphological properties of low-density polyethylene/ultra-high-molecular-weight polyethylene and linear low-density polyethylene/ultra-high-molecular-weight polyethylene blends. *J Appl Polym Sci* **2013**, *129*, 945-953, doi:10.1002/app.38374.
35. Chaudhuri, K.; Poddar, S.; Pol, H.; Lele, A.; Mathur, A.; Rao, G.S.S.; Jasra, R. The effect of processing conditions on the rheological properties of blends of ultra high molecular weight polyethylene with high-density polyethylene. *Polym Eng Sci* **2019**, *59*, 821-829, doi:10.1002/pen.25016.
36. Dordinejad, A.K.; Jafari, S.H.; Khonakdar, H.A.; Wagenknecht, U.; Heinrich, G. Thermorheological behavior analysis of mLLDPE and mVLDPE: Correlation with branching structure. *J Appl Polym Sci* **2013**, *129*, 458-463, doi:10.1002/app.38745.
37. Zimm, B.H.; Stockmayer, W.H. The Dimensions of Chain Molecules Containing Branches and Rings. *J Chem Phys* **1949**, *17*, 1301-1314.
38. Stadler, F.J. Detecting very low levels of long-chain branching in metallocene-catalyzed polyethylenes. *Rheol Acta* **2012**, *51*, 821-840, doi:10.1007/s00397-012-0642-x.
39. Chaudhuri, K.; Lele, A.K. Rheological quantification of the extent of dissolution of ultrahigh molecular weight polyethylene in melt-compounded blends with high density polyethylene. *J Rheol* **2020**, *64*, 1-12, doi:10.1122/1.5113705.
40. Piel, C.; Stadler, F.J.; Kaschta, J.; Rulhoff, S.; Münstedt, H.; Kaminsky, W. Structure-Property Relationships of Linear and Long-Chain Branched Metallocene High-Density Polyethylenes Characterized by Shear Rheology and SEC-MALLS. *Macromol Chem Physic* **2006**, *207*, 26-38, doi:10.1002/macp.200500321.
41. Stadler, F.J.; Karimkhani, V. Correlations between the Characteristic Rheological Quantities and Molecular Structure of Long-Chain Branched Metallocene Catalyzed Polyethylenes. *Macromolecules* **2011**, *44*, 5401-5413, doi:10.1021/ma200550c.

42. Stadler, F.J.; Piel, C.; Kaminsky, W.; Münstedt, H. Rheological characterization of long-chain branched polyethylenes and comparison with classical analytical methods. *Macromol Symp* **2006**, *236*, 209-218, doi:10.1002/masy.200650426.
43. Stadler, F.J.; Piel, C.; Klimke, K.; Kaschta, J.; Parkinson, M.; Wilhelm, M.; Kaminsky, W.; Münstedt, H. Influence of Type and Content of Various Comonomers on Long-Chain Branching of Ethene/α-Olefin Copolymers. *Macromolecules* **2006**, *39*, 1474-1482, doi:10.1021/ma0514018.
44. Bersted, B.H. On the Effects of Very Low-Levels of Long-Chain Branching on Rheological Behavior in Polyethylene. *J Appl Polym Sci* **1985**, *30*, 3751-3765.
45. Stadler, F.J.; Mahmoudi, T. Understanding the effect of short-chain branches by analyzing viscosity functions of linear and short-chain branched polyethylenes. *Korea-Aust Rheol J* **2012**, *23*, 185-193, doi:10.1007/s13367-011-0023-5.
46. Yan, Z.-C.; Stadler, F.J. Classification of thermorheological complexity for linear and branched polyolefins. *Rheol Acta* **2018**, *57*, 377-388, doi:10.1007/s00397-018-1088-6.
47. Stadler, F.J.; Münstedt, H. Numerical description of shear viscosity functions of long-chain branched metallocene-catalyzed polyethylenes. *Journal of Non-Newtonian Fluid Mechanics* **2008**, *151*, 129-135, doi:10.1016/j.jnnfm.2008.01.010.
48. Stadler, F.J.; Münstedt, H. Erratum to “Numerical description of shear viscosity functions of long-chain branched metallocene-catalyzed polyethylenes” [J. Non-Newton. Fluid Mech. 151 (2008) 129–135]. *Journal of Non-Newtonian Fluid Mechanics* **2008**, *153*, 203, doi:10.1016/j.jnnfm.2008.05.001.
49. Kronig, R.D.L. On the theory of dispersion of x-rays. *Journal of the Optical Society of America and Review of Scientific Instruments* **1926**, *12*, 547-557, doi:10.1364/Josa.12.000547.
50. Kramers, H.A. La diffusion de la lumiere par les atomes. In Proceedings of Atti Cong. Intern. Fisica, (Transactions of Volta Centenary Congress), Como; pp. 545-557.
51. Kazatchkov, I.B.; Bohnet, N.; Goyal, S.K.; Hatzikiriakos, S.G. Influence of molecular structure on the rheological and processing behavior of polyethylene resins. *Polym Eng Sci* **1999**, *39*, 804-815.
52. Stadler, F.J.; Münstedt, H. Correlations between the Shape of Viscosity Functions and the Molecular Structure of Long-Chain Branched Polyethylenes. *Macromol Mater Eng* **2009**, *294*, 25-34, doi:10.1002/mame.200800251.
53. Münstedt, H. Dependence of the Elongational Behavior of Polystyrene Melts on Molecular-Weight and Molecular-Weight Distribution. *J Rheol* **1980**, *24*, 847-867.
54. Trinkle, S.; Friedrich, C. Van Gurp-Palmen-plot: a way to characterize polydispersity of linear polymers. *Rheologica Acta* **2001**, *40*, 322-328, doi:10.1007/s003970000137.
55. Trinkle, S.; Walter, P.; Friedrich, C. Van Gurp-Palmen Plot II - Classification of long chain branched polymers by their topology. *Rheologica Acta* **2002**, *41*, 103-113, doi:10.1007/s003970200010.

 doi:10.20944/preprints202012.0561.v1